# Space-momentum correlations in 8 *A*GeV Au+Au collisions*

WU Feng-Juan(吴凤娟) SHAN Lian-Qiang(单连强) FENG Qi-Chun(冯启春) HUO Lei(霍雷)[1)]

Department of Physics, Haerbin Institute of Technology, Haerbin 150001, China

**Abstract** Within the RQMD model, space-momentum correlations, i.e. the correlations between final momentum anisotropy and initial eccentricity, are studied for 8 *A*GeV Au+Au events classified according to the multi-particle azimuthal correlations. The results show that the final elliptic flow fluctuations depend on the initial collision geometry. There are clear space-momentum correlations for nucleons during the whole dynamical evolution of the collisions.

**Key words** space-momentum correlations, elliptic flow fluctuations, initial spatial eccentricity

**PACS** 25.75.Ld, 25.75.Gz

## 1 Introduction

One of the main goals of relativistic heavy-ion collision experiments is to study nuclear matter under the extreme conditions of high densities and high temperatures, i.e. to learn more about the nuclear equation of state (EoS) [1–3]. Anisotropic flow is a motion characterized by space-momentum correlations [4]. There is theoretical evidence that anisotropic flow is very sensitive to the maximal compression reached in the early phase of a heavy ion reaction and hence can provide an important probe for the EoS [5]. However, the anisotropic flow in the final state represents a time integral from the initial condition in the overlap zone to subsequent evolution of the hot matter created in nucleus-nucleus collisions and one cannot get the EoS from the flow directly [6]. Recently, event-by-event elliptic flow fluctuations at RHIC energies have been found to be correlated with the initial shape of the system formed in the early stage of the reaction [7–9]. At low energy, due to the finite number of particles in an event, one can reconstruct a large event by putting many events together for the flow analysis. However, much important information may be lost in the averaging process.

Sorge has argued that a combination of different types of transverse flow observables may allow a more differentiated investigation of the EoS [5]. Furthermore, anisotropic flow is a collective effect, and multi-particle azimuthal correlations can reveal new insights on the space-time evolution of the collective system [10–12]. In this paper, we will study the space-momentum correlations in events classified according to the multi-particle azimuthal correlations in 8 *A*GeV Au+Au collisions within the RQMD model (v2.4, a soft momentum-dependent (SM) mean field code). A detailed description of the RQMD model can be found elsewhere [13].

## 2 Multi-particle azimuthal correlations

Anisotropic flow is commonly characterized by the Fourier coefficients [14]:

$$v_n = \langle \cos n(\phi - \psi_r) \rangle \ , \tag{1}$$

where $\phi$ is the azimuthal angle of the emitted particles in the laboratory coordinate system, and $\psi_r$ is the azimuthal angle of the reaction plane. The angular bracket denotes an average over all particles in a given phase space region and over many events. The first and second coefficients, $v_1$ and $v_2$, characterize the directed and elliptic flow, respectively.

Received 19 January 2009

* Supported by Science Foundation of Harbin Institute of Technology (HIT.2002.47, HIT.2003.33)

1) E-mail: lhuo@hit.edu.cn

One can reconstruct flow vectors $\vec{Q}_n = Q_n \cos n\psi_n \vec{e}_x + Q_n \sin n\psi_n \vec{e}_y$ using the anisotropic flow itself for each event in a certain system [11, 12, 15–17], where the azimuthal angle is in the range of $0 \leqslant n\psi_n < 2\pi$. The observable $\beta = \psi_2 - \psi_1$ is the azimuthal angle between the elliptic and directed flow in each event, and the azimuthal correlation function $C(\beta)$ can be expressed as [12, 16],

$$C(\beta) = A_0[1 + A_{12}\cos 2(\beta + \beta_0)], \qquad (2)$$

where $\beta_0$ characterizes the relative direction of the directed and elliptic flow. The value of $\beta_0$ is close to zero, $\beta_0 \sim 0$, meaning that the elliptic flow is parallel to the directed flow which corresponds to the positive elliptic flow, while $\beta_0 \sim \pi/2$ means the negative elliptic flow. The coefficient $A_{12}$ quantifies the strength of the azimuthal correlations between the directed and elliptic flow, and $A_0$ is a normalization factor.

Figure 1 shows the azimuthal correlation function $C(\beta)$ for nucleons (protons and neutrons) in 8 *A*GeV Au+Au collisions calculated with the RQMD model at impact parameter $b = 6$ fm. In this analysis, we use 50000 simulated events. The vectors $\vec{Q}_1$ and $\vec{Q}_2$ were calculated within the normalized rapidity regions of $|(y/y_{\text{beam}})_{\text{c.m.}}| \geqslant 0.3$ and $|(y/y_{\text{beam}})_{\text{c.m.}}| < 0.3$, respectively. The solid line in Fig. 1 is a fit with Eq. (2). The fitted results are $A_{12} = 0.185 \pm 0.008$ and $\beta_0 = 0.016 \pm 0.022$. This corresponds to the positive elliptic flow. The fact that the curve in Fig. 1 is not flat confirms the multi-particle azimuthal correlations between the two components of the transverse collective motion. It can be seen that the probability of $\beta \sim \pi/2$ is not zero in 8 *A*GeV Au+Au collisions. Fig. 1 reveals that there exist azimuthal angle fluctuations in the collisions [12, 16].

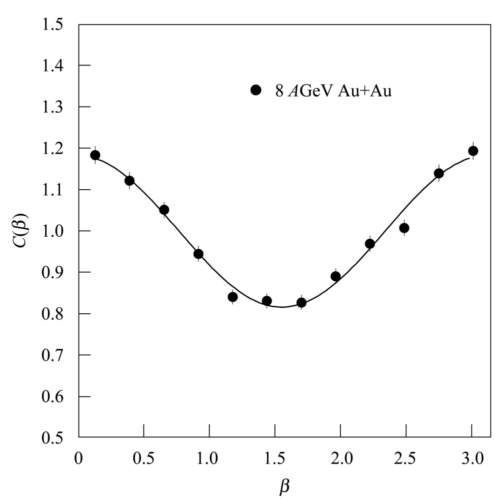


Fig. 1. The azimuthal correlation functions $C(\beta)$ for nucleons from RQMD calculations in 8 *A*GeV Au+Au collisions at $b = 6$ fm. The solid line is a fit with Eq. (2).

## 3 Elliptic flow fluctuations and initial spatial eccentricity

In order to gain more insight into the azimuthal angle fluctuations, we divide the events into different groups according to the multi-particle azimuthal correlations. The azimuthal correlation function $C(\beta)$ is symmetric about $\beta \sim \pi/2$ between 0 and $\pi$, and the range of 0 to $\pi/2$ is divided into six equal intervals. The number of the particles in an event is finite, so we put the events in the same group together to reconstruct six large events for the flow analysis. The elliptic flow $v_2$ for nucleons at mid-rapidity ($|(y/y_{\text{beam}})_{\text{c.m.}}| < 0.3$) calculated from Eq.(1) in 8 *A*GeV Au+Au collisions as a function of the azimuthal angle $\beta$ is shown in Fig. 2. The errors are statistical only and they are smaller than the symbol size. For all events, the average value of the elliptic flow for nucleons at mid-rapidity can be calculated as follows:

$$\langle v_2 \rangle = \int_0^{\pi} C(\beta) v_2(\beta) \mathrm{d}\beta\,. \qquad (3)$$

The average value of the elliptic flow ($\langle v_2 \rangle = 0.015 \pm 0.001$) is positive, which is consistent with experimental data and theoretical research [18, 19]. The incident energy, the impact parameter and the EoS are the same in all events; however, the elliptic flow in the final state is very different in the six groups and it is even negative for three groups with $\beta > \pi/4$.

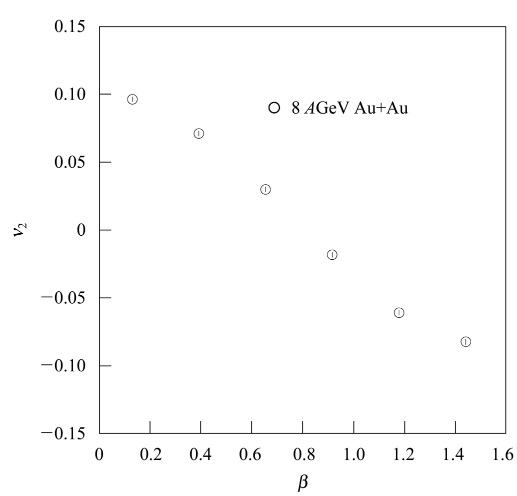


Fig. 2. Elliptic flow for nucleons at mid-rapidity as a function of the azimuthal angle $\beta$ in 8 *A*GeV Au+Au collisions at $b = 6$ fm.

Recent analyses have shown that the final momentum distribution of particles is imprinted by the initial geometrical configuration at RHIC energies, event-by-event, which can be characterized by its spatial eccentricity [7–9]

$$\varepsilon=\frac{\langle y^2-x^2\rangle}{\langle y^2+x^2\rangle}, \quad (4)$$

where $x$ and $y$ are the projections of the participant particle coordinate in and perpendicular to the reaction plane, respectively. In the RQMD model the initial nucleon position in each colliding nuclei is generated according to a Woods-Saxon distribution [20].

Figure 3 shows the distributions of the event-by-event initial spatial eccentricity $\varepsilon$ for events in (a) group ($0\leqslant\beta<\pi/12$) and (b) group ($5\pi/12\leqslant\beta<\pi/2$). $N$ denotes the number of events in the corresponding event group. In the calculation of the initial spatial eccentricity, only those nucleons which will collide with other particles more than one time and the rapidity $|(y/y_{\text{beam}})_{\text{c.m.}}|<0.75$ when they are frozen out are included [21]. The solid curves in Fig. 3 are the Gaussian fits. The average values of the initial spatial eccentricity $\langle\varepsilon\rangle$ are $0.098\pm0.001$ and $0.066\pm0.001$ for the (a) and (b) group, respectively. The widths $\sigma$ of the distributions are $0.088\pm0.001$ and $0.089\pm0.001$ for the (a) and (b) group, respectively. Fig. 3 shows that the average values are different, and large event-by-event fluctuations exist for initial spatial eccentricity in both the (a) and (b) groups.

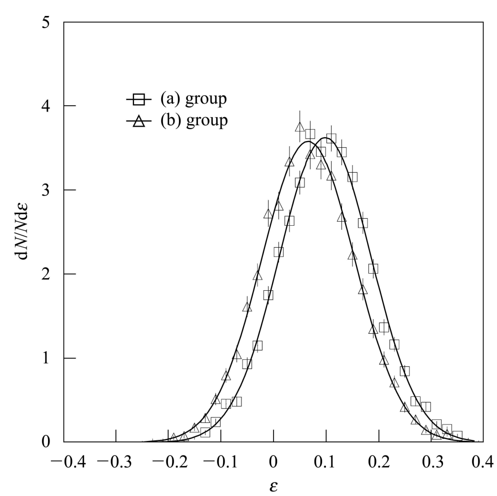


Fig. 3. The distributions of $\varepsilon$ for initial participant nucleons (open squares: (a) group; open triangles: (b) group) in 8 $A$GeV Au+Au collisions at $b$ = 6 fm. The solid curves are the Gaussian fits.

Figure 4 shows the average initial spatial eccentricity $\langle\varepsilon\rangle$ as a function of the azimuthal angle $\beta$ in 8 $A$GeV Au+Au collisions at $b$ = 6 fm. The positive average values of the initial spatial eccentricity imply that the initial participant zone in the different $\beta$ groups is approximately an ellipse, and the spatial density gradients are larger along the short side ($x$ axis) of the ellipse than along the long side ($y$ axis), which gives rise to pressure gradients stronger in-plane than out-of-plane. Furthermore, the average values of the initial spatial eccentricity in the groups with $\beta\sim0$ are larger than those in the groups with $\beta\sim\pi/2$, which means that the pressure gradient ratio of in-plane to out-of-plane in the $\beta\sim0$ groups will be larger than that in the $\beta\sim\pi/2$ groups.

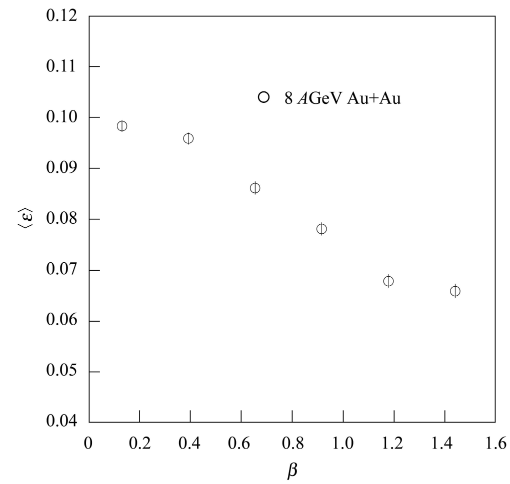


Fig. 4. The average initial spatial eccentricity $\langle\varepsilon\rangle$ as a function of the azimuthal angle $\beta$ in 8 $A$GeV Au+Au collisions at $b$ = 6 fm.

## 4 Time evolution of the space-momentum correlations

Figure 5 shows the time evolution of the spatial eccentricity $\varepsilon$ for the participant nucleons and the elliptic flow $v_2$ for mid-rapidity nucleons in 8 $A$GeV Au+Au collisions ($b$ = 6 fm). Here the spatial eccentricity is calculated from the coordinates of the nucleons which participate in the collisions at time $t$. The nucleons move on a straight line trajectory after the last collision. The open circles represent the results calculated for all events, the open squares for the (a) group ($0\leqslant\beta<\pi/12$) and the open triangles for the (b) group ($5\pi/12\leqslant\beta<\pi/2$). Note that only the statistical errors are given.

From Fig. 5 one observe that the spatial eccentricity $\varepsilon$ first increases and then decreases with time. The dense and hot participant region is gradually formed from the beginning of the reaction to the maximum overlap of the projectile and target nucleus. The spatial eccentricity of the (a) group is slightly larger than that of the (b) group from the beginning of the reaction during the compression stage, so the expansion of the (a) group will be a little faster than that of the (b) group in the subsequent dynamical evolution of collisions. The transverse expansion will lead to a decrease in the system spatial anisotropy and therefore to an increase in the elliptic flow signal.

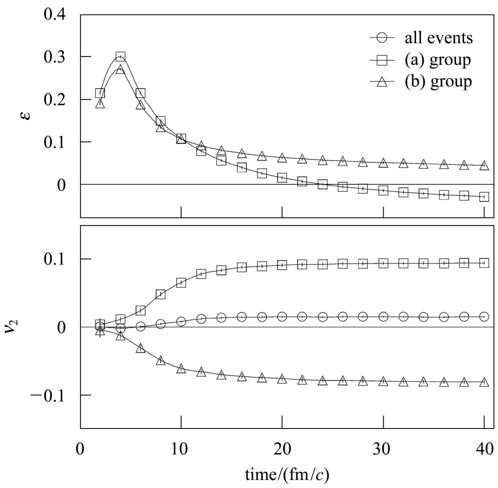


Fig. 5. Time evolution of the spatial anisotropy $\varepsilon$ for the participant nucleons and the elliptic flow $v_2$ for nucleons at mid-rapidity ($|(y/y_{\rm beam})_{\rm c.m.}| < 0.3$) calculated with RQMD in 8 $A$GeV Au+Au collisions ($b = 6$ fm). The open circles represent all events, the open squares (a) group and the open triangles (b) group.

During the compression stage, the longitudinal kinetic energy is converted into thermal and potential compression energy. Since the pressure gradients in the in-plane direction are the largest, there are more particles preferentially emitted in the reaction plane than out-of-plane; however, the spectators will shadow its emission. For all events, there is no visible elliptic flow from the beginning of the reactions, and subsequently the elliptic flow reaches saturation at around 15 fm/$c$. The time dependence of the elliptic flow in the (a) and (b) groups is quite different. The sign of the elliptic flow generated in the (a) group is always positive, which corresponds to more particles in-plane than out-of-plane, and the average spatial eccentricity decreases quickly with time. On the other hand, the sign of the elliptic flow generated in the (b) group remains negative, which is associated with preferential particle emission perpendicular to the reaction plane, and the average spatial eccentricity decreases slowly with time. There are clear space-momentum correlations during the collective expansion of the system.

## 5 Conclusion

In this paper we have investigated the space-momentum correlations in events classified according to the multi-particle azimuthal correlations between the directed and elliptic flow for Au+Au collisions at 8 $A$GeV within the RQMD model (v2.4, SM mean field code). The results show that the elliptic flow fluctuations depend on the initial geometrical configuration. On average, the sign of elliptic flow for nucleons is positive in 8 $A$GeV Au+Au collisions; however, it remains negative in the (b) group of events during the whole dynamical evolution of collisions. The initial spatial eccentricity and the collective transverse expansion of the system affect the particle azimuthal distribution in momentum space, and space-momentum correlations develop.

### References

1 Danielewicz P, Lacey R, Lynch W G. Science, 2002, **298**: 1592–1596
2 Hartnack C, Oeschler H, Aichelin J. Phys. Rev. Lett., 2006, **96**: 012302
3 Henning W F. Nucl. Phys. A, 2008, **805**: 502c–510c
4 Snellings R J M, Sorge H, Voloshin S A et al. Phys. Rev. Lett., 2000, **84**: 2803–2805
5 Sorge H. Phys. Rev. Lett., 1997, **78**: 2309–2312
6 Kolb P F, Sollfrank J, Heinz U. Phys. Lett. B, 1999, **459**: 667–673
7 Alver B, Back B B, Baker M D et al. (PHOBOS Collaboration). Phys. Rev. C, 2008, **77**: 014906; Abelev B I, Aggarwal M M, Ahammed Z et al. (STAR Collaboration). Phys. Rev. C, 2008, **77**: 054901
8 Miller M, Snellings R. arXiv: nucl-ex/0312008
9 Bhalerao R S, Ollitrault J Y. Phys. Lett. B, 2006, **641**: 260–264
10 Borghini N, Dinh P M, Ollitrault J Y. Phys. Rev. C, 2000, **62**: 034902; 2001, **63**: 054906; 2001, **64**: 054901
11 HUO Lei, ZHANG Wei-Ning, CHEN Xiang-Jun et al. HEP & NP, 2003, **27**(1): 53–57 (in Chinese)
12 WU Feng-Juan, SHAN Lian-Qiang, ZHANG Jing-Bo et al. J. Phys. G, 2009, **36**: 015112
13 Sorge H. Phys. Rev. C, 1995, **52**: 3291–3314
14 Voloshin S A, ZHANG Y. Z. Phys. C, 1996, **70**: 665–671
15 HUO Lei, ZHANG Jing-Bo, ZHANG Wei-Ning et al. HEP & NP, 2003, **27**(3): 249–252
16 WU Feng-Juan, SHAN Lian-Qiang, ZHANG Jing-Bo et al. Chin. Phys. C (HEP & NP), 2008, **32**(12): 984–988
17 Poskanzer A M, Voloshin S A. Phys. Rev. C, 1998, **58**: 1671–1678
18 Pinkenburg C, Ajitanand N N, Alexander J M et al. Phys. Rev. Lett., 1999, **83**: 1295–1298
19 LIU H, Ajitanand N N, Alexander J M et al. Nucl. Phys. A, 1998, **638**: 451c–454c
20 Voloshin S A, Poskanzer A M. Phys. Lett. B, 2000, **474**: 27–32
21 Sood A D, Puri R K. Phys. Rev. C, 2004, **70**: 034611